A certifiable resource allocation for real-time multi-hop 6TiSCH wireless networks

Qi Wang, Katia Jaffrès-Runser, Yongjun Xu, Jean-Luc Scharbarg

A certifiable resource allocation for real-time multi-hop 6TiSCH wireless networks

Qi Wang *, Katia Jaffrès-Runser†, Yongjun Xu *, Jean-Luc Scharbarg†
*Institute of Computing Technology, Chinese Academy of Sciences, Beijing, CHINA
Email: {wangqi08, xyj}@ict.ac.cn
†Université de Toulouse, IRIT / ENSEEIHT, F-31061, Toulouse, FRANCE
Email: {katia.jaffres-runser, jean-luc.scharbarg}@irit.fr

***Abstract*—In safety-related industrial systems, stringent timelines and a high degree of reliability in communications are required. Networking protocols have to be certified using a mathematical framework that ascertains the end-to-end communication delay of flows is upper bounded. The recently created IETF 6TiSCH networking stack is a promising candidate to offer real-time communication services as communications are scheduled at the link layer in time and frequency. Its 6top sublayer manages the way communication resources are scheduled and thus messages routed. This paper proposes a novel certifiable resource allocation algorithm for multi-hop 6TiSCH wireless networks that simultaneously offers high reliability, low end-to-end delay and low energy consumption for safety-related industrial applications. The schedules are defined such as to directly derive a bound on the worst-case end-to-end delay. Schedules are fixed and computed by solving a multi-objective optimization problem. Two different problems are defined. The first one designs a deterministic schedule and the other one a probabilistic schedule where node are assigned a probability to forward a message in a TSCH cell. We show in our results that the latter method offers better performance in terms of robustness as possible losses due to fading are compensated for by cyclic path redundancies.**

***Keywords*—resource allocation, probabilistic worst-case end-to-end delay, network reliability, TSCH**

I. Introduction

Wireless multi-hop networks (i.e., sensor and mesh networks) will be increasingly employed in safety-related industrial systems, such as factory automation, industrial surveillance and monitoring of nuclear plants, due to their appealing ease of deployment and scalability. In order to ensure safety, time evolution of such systems is constrained by strict deadlines and requires a high degree of reliability in communication. For wireless networks to be deployed in such systems, deterministic wireless communications have to be guaranteed.

Several wireless protocols have been designed recently to offer mainly real-time garanties: WirelessHART [1], ISA100.11a [2], and IEEE802.15.4e [3]. They are based on wireless short-range communication technologies and offer time-slotted channel hopping medium access. While WirelessHART and ISA100.11a define a complete protocol stack, IEEE802.15.4e only defines the physical layer and three distinct Medium Access Control (MAC) layers: Low Latency Deterministic Network (LLDN), time-frequency blocked Channel Hopping (TSCH), and Deterministic and Synchronous Multichannel Extension (DSME). Among these, TSCH is the one facilitating multi-hop operations, and is able to cope efficiently with external interference and multiple fading channels. The clean layering allows IEEE802.15.4e TSCH to fit under an IPv6-enabled protocol stack for low-power wireless networks, which was recently proposed by the IETF 6TiSCH working group.

The IETF 6TiSCH working group has defined the 6TiSCH operation Sublayer (6top) [4] as the next upper layer of the TSCH MAC (IEEE802.15.4e MAC-TSCH). This 6top sublayer manages the way communication resources are scheduled in time and frequency, while monitoring performance and collecting statistics at each node to further optimize routes and channel access. To allow maximum flexibility, the scheduling policy is not standardized by 6TiSCH. Scheduling can thus be implemented in a centralized or a distributed manner. Schedules can be pre-calculated or adjusted dynamically to new demands. Several scheduling policies for 6TiSCH have been designed, but only few of them offer a bounded worst case delay calculation method. Domingo-Prieto et al. [5] propose a distributed and dynamic scheduling policy where each node determines the number of cells to schedule according to its traffic demand. Duquennoy et al. propose a best-effort decentralized scheduling approach named Orchestra [6] that randomly allocates slots without requiring control messages to be exchanged by nodes. Recently, Hosni et. al. [7] have proposed a distributed algorithm to schedule the transmissions while upper bounding the end-to-end delay by the slot frame size. More specifically, their solution guarantees that the maximum end-to-end delay equals to the slot frame duration. Their scheduling policy reduces the end-to-end delay by allocation more cells to a communication but this over-provisioning increases both the number of collisions and the energy consumption.

This paper proposes a novel certifiable resource allocation algorithm for multi-hop 6TiSCH wireless networks that offers high communication reliability, low end-to-end delay and low energy consumption for safety-related industrial applications. Our scheduling policy pre-calculates the schedules using a novel multi-objective optimization framework where network reliability, end-to-end delay and energy consumption are optimized for each multi-hop flow. Our schedule is directly derived from the performance metrics of the flows, all extracted from a cross-layer Markov-based performance model of the multi-hop wireless network. From this cross-layer framework, we can derive the end-to-end delay distribution for each flow. This distribution can be leveraged to calculate a probabilistic

worst-case end-to-end delay bound and thus, properly certify the communication delay.

This novel framework is the extension of our previous works [8], [9], [10] to the 6TiSCH scheduling problem. Unique to the present work, is the definition of the closed-form expressions for network reliability which measures the probability to receive one frame over a multihop path. Another addition is the derivation of the delay distribution of the first arrived frames. Indeed, multi-path communications can be defined in our framework and previous delay distributions would be computed for all received messages, including redundant copies traveling on different paths. Derivations of this paper only account for the frames arrived first, and not for subsequent copies.

This paper underlines two different implementations of our framework. The first one is fully deterministic in its essence as scheduling decisions are deterministic. The second one is stochastic as scheduling decisions are given by forwarding probabilities. Unique to this stochastic scheduling policy, redundancy can be adjusted such as to prove, given a realistic channel model, that maximum reliability is achieved and end-to-end delays are bounded. This redundancy is enforced naturally by the stochastic decisions of the nodes resulting in copies being carried over cyclic paths in the network. In this paper, we highlight in our results how cyclic paths can positively impact the overall performance of our scheduling under bad channel conditions.

To summarize, the main contributions of our work are the following ones: i) the definition of a wireless multi-hop (possibly multi-path) cross-layer network performance framework that captures reliability, end-to-end delay and energy consumption of flows, ii) a 6TiSCH offline static scheduling multi-objective (MO) algorithm that optimizes concurrently the aforementioned performance metrics and iii) a comparison of a deterministic and a probabilistic schedule implementation of our scheme for two core multi-hop networking topologies.

This paper is organized as follows. Section II introduces our system model and the node scheduling algorithm. Section III introduces our cross-layer model and the related reliability, end-to-end delay and energy performance metrics. Calculation of the end-to-end delay distribution is given as well for a given flow. Section IV formulates the MO optimization problem that derives optimal forwarding probabilities for resource allocation. Section V validates the performance of algorithm against simulation for the deterministic and stochastic study cases. Section VI concludes this paper.

II. System model and algorithm

A. Multihop topologies

In this work, we still investigate two different atomic topologies [9] that are at the core of many deployment scenarios of wireless multi-hop communications. We will concentrate first on a linear deployment scenario as shown in Fig. 1(a). In this example, relay R_1 can only communicate with R_2 in both ways. R_1 can not send frames to S and D can only receive frames from R_3. The second 2-flow / 2-relay topology has been investigated to capture the contention effect of a set of nodes carrying multiple flows. The first flow is emitted by S_1 going to D_1 and the second flow is emitted by S_2, going to D_2. This situation is critical since the relays have to listen to both flows and to re-emit them concurrently.

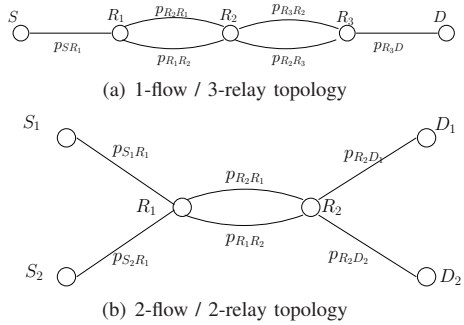

(a) 1-flow / 3-relay topology

(b) 2-flow / 2-relay topology

Fig. 1. Investigated topologies: (a) Linear topology composed of one flow and 3 relay nodes ; (b) Crossflow topology with 2 flows.

Source nodes generate strictly periodic flows of frames. As explained later in Section V, the frame generation period is set such as to have only one frame in the emission buffer of the source at all times. Thus, the only delay we are computing analytically or measuring by simulation is the MAC delay, i.e. the time for the frame to gain access to the channel. There is no delay related to queuing in this work.

B. Network model and algorithm

IEEE802.15.4e [3] is an amendment to the MAC protocol of IEEE802.15.4-2011 [11]. The Time Synchronized Channel Hopping (TSCH) mode of IEEE802.15.4e yields ultra-high reliability and low-power operations. All sensor in a IEEE802.15.4e network are synchronized. Time is split into time slot, each typically 10ms long. Time slots are grouped into a slotframe, which continuously repeats over time, as shown in Fig. 2. TSCH doesn't impose a slotframe size. Depending on the application needs, the slotframe size can range from 10's to 1000's of time slots. In consecutive slotframe cycles, the same channel offset translates into a different communication frequency, resulting in channel hopping. The number of available channels is 16 when using radios that are compliant with IEEE 802.15.4 at 2.4GHz. The TSCH schedule can be represented by a 2-D matrix of width the number of slots in a slotframe, and height the number of available channels. Each element in the matrix is called a "cell" (we use as well the term "time-frequency block" interchangeably in this paper). A cell is scheduled to instruct each node what to do, either to transmit or receive.

As seen in Fig. 1, there are bi-directional links between relays and destinations. It is a way to represent multiple paths, by allowing cyclic paths (loop paths) with different lengths. With path diversity, a frame can travel multiple paths to the destination, giving additional redundancy to further increase the communication reliability.

Each relay node is characterized by a set of *forwarding probabilities* x_{ij}^{uv}, which govern its forwarding decisions. These forwarding probabilities are optimized later to define a global schedule at using Algorithm 1. Assuming node j receives a frame from node i in the current slotframe s on cell u, it decides to forward this frame on cell v of stotframe $s+1$

with probability x_{ij}^{uv}. As such, a frame may travel of one hop in the duration of *at most* one slotframe. Node j only re-emits at most once a frame received in slot u as $\sum_v x_{ij}^{uv} \leq 1$. In case $\sum_v x_{ij}^{uv} < 1$, the frame may be dropped with probability $1 - \sum_v x_{ij}^{uv}$.

We will first investigate the performance of scheduling policy by optimizing binary forwarding probabilities (i.e. chosen to be 0 or 1). This optimisation step creates a deterministic schedule. Secondly, the search is performed for real forwarding probabilities that belong to the continuous set [0,1]. In this implementation, the schedule is stochastic. We show that in this context, the definition of cyclic paths can further improve reliability by adding path diversity to the multi-hop transmission.

Algorithm 1 Resource allocation of node j in cell u for a multihop 6TiSCH wireless networks.

```
if memory of cell u not empty then
  Send the frame;
else
  if node j receives a frame p from i in time-frequency
  block u then
    Generate a random value x ∈ [0, 1];
    for each time-frequency block v ∈ T, v ≠ u do
      if v==1 and x ≤ x_ij^u1 then
        Store the frame p into memory of time-frequency
        block 1;
      else
        if x_ij^u(v−1) ≤ x ≤ x_ij^uv then
          Store the frame p into memory of time-
          frequency block v;
        end if
      end if
    end for
  end if
end if
```

Each node of the network is represented as well by its emission rate in a slot. The emission rate τ_i^u represents the proportion of time a node i is active in a slot u, in average. For instance, a value of $\tau_i^u = 0.5$ means that node i is emitting in slot u every two slotframes. Source nodes have an emission rate of 1 in time-frequency block 1 for both topologies.

To ensure flow conservation and capture the cross-layer effect, relay nodes have an emission rate that is proportional to the amount of frames they receive from other nodes and their respective forwarding probabilities. The amount of frames they receive is a function of the number of frames other nodes have sent, and the link quality over which they have been received. The link quality is quantified by a channel probability p_{ij}^u that represents the chances for a frame to be properly received in time-frequency block u over link (i, j). This channel probability is derived from the average frame Error Rate (PER) on link (i, j) and from the emission rates of sending nodes. (*cf.* [8] for details). Only interference of nodes that share the same time-frequency block are accounted for in our model. To calculate the PER, any channel model can be fed into our calculations to retrieve realistic results.

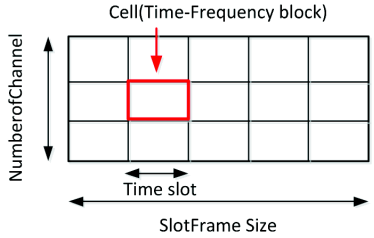

Fig. 2. IEEE802.15.4-TSCH mode - illustration of a slotframe with 5 time slots and number of 3 channel.

Flow conservation is ensured if the following set of $|E|$ equations are valid:

$$\sum_{(i,j)\in\overrightarrow{\mathcal{N}_j}} \sum_{u\in\mathcal{T}} \tau_i^u p_{ij}^u x_{ij}^{uv} = \tau_j^v, \quad \forall (j,v) \in E \tag{1}$$

where $\tau_i^u p_{ij}^u$ is the probability that a frame sent by i on time-frequency block u arrives in j. $|E|$ is given by the number of edges times the number of time-frequency blocks. $\overrightarrow{\mathcal{N}_j^v}$ is the set of outgoing edges coming into node j from any node i on u. We refer the reader to [9] for more details.

III. Analytical performance framework

This section introduces our framework that helps us in defining performance criteria (e.g. reliability, end-to-end delay and energy consumption) and calculate the end-to-end delay distribution for any flow of the network. This framework derives a mathematical Markov-like network model that accounts for the forwarding probabilities (i.e. our scheduling decisions) and the wireless channel statistics associated to these forwarding probabilities. It is illustrated for the 2-flow / 2-relays topology of Fig. 1.

A. Relaying and arrival matrices

The relaying matrix Q gives the probabilities for any emission (i, u) in slotframe s to be emitted as (j, v) at the following slotframe $(s+1)$ by the relays of the networks. The arrival matrix $\mathcal{A}$ is composed of the probabilities to go from any transient state to any absorbing state, i.e. the probabilities for any emission (i, u) at slotframe s to arrive at a destination D_j in time-frequency block v at slotframe $(s + 1)$.

1) The relaying matrix Q:

$$Q = \begin{bmatrix} 0 & Q_{12} & \cdots & Q_{1N} \\ Q_{21} & 0 & \cdots & Q_{2N} \\ \vdots & & & \vdots \\ Q_{N1} & \cdots & Q_{N-1N} & 0 \end{bmatrix}$$

0 is a $|T|$-by-$|T|$ zero matrix representing the fact that node i never forwards a frame to itself. $|T|$ is the number of time-frequency blocks. N is the number of relays. A reduced version of Q can be defined where only the relays that belong to a given path $\mathbf{p}$ are accounted for. This sub-matrix $Q_{sub}(\mathbf{p})$ keeps the values $Q_{ij}(i, j \in \mathbf{p})$ and sets other elements to 0.

The matrix Q_{ij} is a $|T|$-by-$|T|$ matrix that gives the probabilities of j to transmit a frame sent by node i for all

possible combinations of time-frequency blocks:

$$Q_{ij} = \begin{bmatrix} Q_{ij}^{11} & \cdots & Q_{ij}^{1|T|} \\ \vdots & & \vdots \\ Q_{ij}^{|T|1} & \cdots & Q_{ij}^{|T||T|} \end{bmatrix} \quad (2)$$

where Q_{ij}^{uv} is the probability for a node j to retransmit on time-frequency block v a frame that has been transmitted by node i on time-frequency block u. From our network model, it equals to $Q_{ij}^{uv} = p_{ij}^{u} x_{ij}^{uv}$.

2) The arrival matrix $\mathcal{A}$:

$$\mathcal{A} = \begin{bmatrix} \mathcal{A}_{1D_1} & \cdots & \mathcal{A}_{1D_{|\mathcal{D}|}} \\ \vdots & & \vdots \\ \mathcal{A}_{ND_1} & \cdots & \mathcal{A}_{ND_{|\mathcal{D}|}} \end{bmatrix}$$

$\mathcal{A}_{iD_j}$ is a $|T|$-by-$|T|$ diagonal matrix whose diagonal elements $\mathcal{A}_{iD_j}^{u}$ give the probabilities for a frame transmitted by a node i in time-frequency block u to arrive at destination D_j and $\mathcal{A}_{iD_j}^{u} = p_{iD_j}^{u}$.

Q_S and $\mathcal{A}_S$ are the relaying and arrival matrices for the frames sent by the sources. We have

$$Q_S = \begin{vmatrix} Q_{S_1 1} & .. & Q_{S_1 N} \\ \vdots & & \vdots \\ Q_{S_{|\mathcal{O}|}1} & .. & Q_{S_{|\mathcal{O}|}N} \end{vmatrix} \mathcal{A}_S = \begin{vmatrix} \mathcal{A}_{S_1 D_1} & .. & \mathcal{A}_{S_1 D_{|\mathcal{D}|}} \\ \vdots & & \vdots \\ \mathcal{A}_{S_{|\mathcal{O}|} D_1} & .. & \mathcal{A}_{S_{|\mathcal{O}|} D_{|\mathcal{D}|}} \end{vmatrix}$$

where $Q_{S_i j}$ follows the pattern given by (2) and $\mathcal{A}_{S_i D_j}$ is a $|T|$-by-$|T|$ diagonal matrix whose diagonal elements are $\mathcal{A}_{S_i D_j}^{u} = p_{S_i D_j}^{u}$. $|\mathcal{O}|$ is the number of sources. Matrices are illustrated next for a basic schedule defined for the 2-flow / 2-relays topology.

3) Illustration for 2-relay / 2-flow topology: For this scenario, we present the matrices for a schedule where only $|T| = 4$ cells are set: sources S_1 and S_2 transmit in cell 1 and cell 2, respectively ; relays R_1 and R_2 transmit in cell 3 and 4, respectively. Frames are only allowed to loop between relays R_1 and R_2. As such, the shortest path is made of $h_{min} = 3$ hops. Relaying Q and arrival matrix $\mathcal{A}$ are given as follows (diagonal elements of Q are directly set to 0 since relays don't send data to themselves):

$$Q = \begin{bmatrix} 0 & Q_{R_1 R_2}^{34} \\ Q_{R_2 R_1}^{43} & 0 \end{bmatrix}$$

$$= \begin{bmatrix} 0 & p_{R_1 R_2}^{3} x_{R_1 R_2}^{34} \\ p_{R_2 R_1}^{4} x_{R_2 R_1}^{43} & 0 \end{bmatrix}$$

and

$$\mathcal{A} = \begin{bmatrix} \mathcal{A}_{R_1 D}^{3} & 0 \\ 0 & \mathcal{A}_{R_2 D}^{4} \end{bmatrix} = \begin{bmatrix} p_{R_1 D}^{3} & 0 \\ 0 & p_{R_2 D}^{4} \end{bmatrix}$$

The relaying and arrival matrices Q_S for frames sent by S are defined as:

$$Q_S = \begin{bmatrix} Q_{S_1 R_1}^{13} & Q_{S_1 R_2}^{14} \\ Q_{S_2 R_1}^{23} & Q_{S_2 R_2}^{24} \end{bmatrix}$$

where $Q_{S_i R_j}^{uv} = p_{S_i R_j}^{u} x_{S_i R_j}^{uv}$.

B. Network reliability

From this stochastic network model, we can define several performance criteria [8], [9], [10]. Unique to this paper, we define a network reliability criterion that calculates the probability of a frame to arrive at a destination. It is equivalent to the success rate of a frame sent by the source. In this derivation, we account for the probability for a message to arrive on the direct path using the minimum number of hops and, in case the message doesn't arrive on this direct path, we allow frames to loop for h_{max} hops within a cyclic path to further improve communication robustness. For instance, in the 1-flow / 3-relays topology, frames can either arrive using the direct 4-hop path $\{(S, R_1)(R_1, R_2)(R_2, R_3)(R_3, D)\}$. We can allow frames sent by R_2 to be overheard by R_1 such as to be re-emitted by R_1 in the next slotframe, providing a redundant transmission. As such, we can combat fading on the link between R_1 and R_2.

Our reliability criterion is defined with the assumption that at most one cycle located at the k^{th} relay may exist (it means R_k can overhear frames emitted by R_{k+1}). For all other relays, cycles can't exist: all forwarding probabilities going back to the source are set to zero. Intuitively, it is beneficial to set this cycle at the first relay R_1 to compensate for losses arriving early in the path.

Let $\mathcal{P}$ be the set of all possible paths between S_i and D_j. Next, we assume that relay R_{k+1} can overhear R_k. Let h_p be the number of hops of the direct path and h_{max} the maximum number of hops allowed in the communication, with $h_{max} \geq h_p$. The frame transmission can succeed after h_p hops (direct path), after h_{p+2} hops if the frame loops in the cyclic path once, after $h_{p+2\ell}$ if it loops in the cyclic path ℓ times.

The reliability for a given path $\mathbf{p}$ can be defined as:

$$f_R(S_i, D_j) = 1 - \prod_{\mathbf{p} \in \mathcal{P}} [1 - P_{success}(\mathbf{p})] \quad (3)$$

with $P_{success}(\mathbf{p})$ the probability of success on path $\mathbf{p}$ ending in destination D_j which is given by:

$$P_{success}(\mathbf{p}) = \sum_{h=h_p}^{h_{max}} P_{1\text{st}}(h, \mathbf{p})$$

where $P_{1\text{st}}(h, \mathbf{p})$ is the probability for the first frame to arrive in h hops at D_i on path $\mathbf{p}$. To clarify notations, $\mathbf{p}$ is only explicitly mentioned in $P_{1\text{st}}$ if needed. On the direct path, $h = h_p$, and h_{max} is the maximum number of hops a frame needs at the steady state of the Markov chain. Frames forwarded by the relays disappear after at most h_{max} slotframes have elapsed. Thus h_{max} is determined when the difference of the flow rate is arbitrarily small: $(\overrightarrow{\mathcal{F}_R}(1)Q^{h_{max}} - \overrightarrow{\mathcal{F}_R}(1)Q^{h_{max}-1}) <= \delta$ (e.g. $\delta = 10^{-11}$). $\overrightarrow{\mathcal{F}_R}(1)$ is the outgoing flow of relays at the first time frame. It equals to $\overrightarrow{\mathcal{F}_R}(1) = S_m \cdot Q_S$, where S_m is the transmission rate vector of sources.

When $h = h_p$, the first frame to arrive at the destination uses the direct path. This success probability is given by:

$$P_{1\text{st}}(h_p) = S_m \cdot I_S(S_i) \cdot Q_S \cdot Q_{sub}(\mathbf{p})^{h_p - 2} \cdot \mathcal{A} \cdot I_D(D_j)$$

where $I_S(S_i)$ (resp. $I_D(D_j)$) is a selection vector of dimension $|\mathcal{O}||\mathcal{T}|$ (resp. $|\mathcal{D}||\mathcal{T}|$) where the $|\mathcal{T}|$ elements relative

to source S_i (resp. destination D_j) are equal to 1 and the others are equal to 0. Q_S, $Q_{sub}(\mathbf{p})$ are source and relaying matrices for path $\mathbf{p}$. $I_D(D_j)$ accumulates the frame arrival rate in each time-frequency block at destination D_j. S_m is the vector of emission rates of all sources, where $S_m = \left[\begin{array}{cccccccc} \tau^1_{S_1} & \dots & \tau^{|\mathcal{T}|}_{S_1} & \dots & \tau^1_{S_{|\mathcal{O}|}} & \dots & \tau^{|\mathcal{T}|}_{S_{|\mathcal{O}|}} \end{array} \right]$.

When the first frame to arrive at the destination loops once in the cyclic path, we have $h = h_p + 2$. In this case, the transmission of the frame carried by the direct path failed between R_{k+1} and D_j, but the transmission of the first copy created in the loop succeeds. As such, the success probability is in this case :

$$P_{1\text{st}}(h_p + 2) = P_{success}(h_p + 2) \cdot P_{\text{loss}}$$

with $P_{success}(h_p + 2) = P_{1\text{st}}(h_p) \cdot Q^{u_k v_{k+1}}_{k(k+1)} Q^{u_{k+1} v_k}_{(k+1)k}$. The probability P_{loss} to loose the first frame between R_{k+1} and D_j is given by:

$$P_{\text{loss}} = 1 - Q^{u_{k+1} v_{k+2}}_{(k+1)(k+2)} Q^{u_{k+2} v_{k+3}}_{(k+2)(k+3)} \cdots Q^{u_{N-1} v_N}_{(N-1)(N)} p^{u_N}_{N D_j}$$

If the first frame to arrive at the destination loops ℓ times in the cyclic path, we have $h = h_p + 2\ell$.

$$P_{1\text{st}}(h_p + 2\ell) = P_{1\text{st}}(h_p) \cdot \left(Q^{u_k v_{k+1}}_{k(k+1)} Q^{u_{k+1} v_k}_{(k+1)k} \cdot P_{\text{loss}} \right)^{\ell}$$

In this case, $\ell - 1$ first frames get lost but the ℓ^{th} one arrives.

To summarize, the end-to-end network reliability for the flow emitted at S_i and arriving at D_j is given by:

$$\begin{array}{rl} f_R(S_i, D_j) = & 1 - \prod_{\mathbf{p} \in \mathcal{P}} \left[1 - \sum_{\ell=0}^{\ell_{max}} P_{1\text{st}}(h_p, \mathbf{p}) \times \right. \\ & \left. \left(P_{\text{loss}} \cdot Q^{u_k v_{k+1}}_{k(k+1)} Q^{u_{k+1} v_k}_{(k+1)k} \right)^{\ell} \right] \end{array} \quad (4)$$

with $\ell_{max} = (h_{max} - h_p)/2$ the maximum number of times a frame can loop in the cycle located at relay R_k.

If several sources emit a flow to D_j, the network reliability $f_R(D_j)$ at destination D_j is given by:

$$f_R(D_j) = \sum_{i=1}^{|\mathcal{O}|} f_R(S_i, D_j) \quad (5)$$

1) Illustration for 2-relay / 2-flow topology: The reliability criterion is illustrated for this topology. We recall that the cyclic path is located at R_1. First, $f_R(S_1, D_1)$ and $f_R(S_2, D_2)$ are derived as:

$$\begin{array}{rl} f_R(S_1, D_1) = & \sum_{\ell=0}^{\ell_{max}} \tau^1_{S_1} Q^{13}_{S_1 R_1} Q^{34}_{R_1 R_2} p^4_{R_3 D_1} \times \\ & \left(P_{\text{loss}}(D_1) \cdot Q^{43}_{R_2 R_1} Q^{34}_{R_1 R_2} \right)^{\ell} \end{array} \quad (6)$$

where $P_{\text{loss}}(D_1) = (1 - p^4_{R_2 D_1})$.

$$\begin{array}{rl} f_R(S_2, D_2) = & \sum_{h=h_p}^{h_{max}} \tau^1_{S_2} Q^{23}_{S_2 R_1} Q^{34}_{R_1 R_2} p^4_{R_3 D_2} \times \\ & \left(P_{\text{loss}}(D_2) \cdot Q^{43}_{R_2 R_1} Q^{34}_{R_1 R_2} \right)^{\ell} \end{array} \quad (7)$$

where $P_{\text{loss}}(D_2) = (1 - p^4_{R_2 D_2})$.

The overall reliability for the flows ending at D_1 is of $f_R(D_1) = f_R(S_1, D_1) + f_R(S_2, D_1)$. A similar derivation holds for $f_R(D_2)$.

C. Delay metric and delay distribution

In our model, the delay is measured in hops. A frame may travel over several paths, each one of different length in number of hops. It takes at most one slotframe duration for the frame to travel one hop further. So all metrics of delay are expressed in hops, and can be easily converted in time units by multiplying them by $M \times \varsigma_{slot}$, with M the slotframe size and ς_{slot} the slot duration.

The end-to-end delay distribution $P[d_j = h]$ is the probability for a transmission towards D_j to be done in h hops. Thus, from previous derivations, we have the probability mass function (PMF) for the end-to-end delay given by

$$P[d_j = h] =$$

$$\left\{ \begin{array}{ll} \left(1 - \prod_{\mathbf{p} \in \mathcal{P}} \left[1 - P_{1\text{st}}(h_p, \mathbf{p}) \right] \right) / f_R(S_i, D_j) & h = h_p \\ (1 - \prod_{\mathbf{p} \in \mathcal{P}} (1 - \sum_{\ell=0}^{\frac{h-h_p}{2}} P_{1\text{st}}(h_p, \mathbf{p}) \times \\ \left(P_{\text{loss}} \cdot Q^{u_k v_{k+1}}_{k(k+1)} Q^{u_{k+1} v_k}_{(k+1)k} \right)^{\ell}) / f_R(S_i, D_j) & \forall h > h_p \end{array} \right. \quad (8)$$

Here, redundant frame copies that successfully arrive at D_j are not accounted for. The average end-to-end delay $f_D(S_i, D_j)$ is computed by:

$$f_D(S_i, D_j) = \sum_{h=1}^{h_{max}} h * P[d_j = h] \quad (9)$$

1) Illustration for 2-relay / 2-flow topology: Since it is a symmetric topology, the delay distribution is given by

$$P[d_1 = h] = P[d_2 = h] =$$

$$\left\{ \begin{array}{ll} P_{1\text{st}}(h_p) / f_R(D_1) & h = h_p \\ ((\tau^1_{S_1} Q^{13}_{S_1 R_1} + \tau^2_{S_2} Q^{13}_{S_2 R_2}) Q^{34}_{R_1 R_2} [P_{\text{loss}}(D_1) \cdot \\ Q^{43}_{R_2 R_1} Q^{34}_{R_1 R_2})^{\frac{h-(N+1)}{2}} p^4_{R_2 D_1} \Big] / f_R(D_1) & \forall h > h_p \end{array} \right. \quad (10)$$

D. Worst-case delay

A stochastic *worst-case delay* bound [9] for the flow ending at destination D_j is defined as the delay d^w for which the probability $P[d_j \geq d]$ to find a delay larger than d^w is arbitrarily small (for instance smaller than $\delta = 10^{-9}$). Formally, for a flow ending at D_j:

$$d^w = \max \; d \quad s.t. \quad P[d_j \geq d] \leq \delta \quad (11)$$

If several flows exist, it is possible to calculate the worst-case delay for all the flows, which is given by the maximum of the d^w values calculated for all possible destinations.

E. Energy Consumption

We consider as a first approximation that the main energy consumption factor is due to the emission and reception of a frame. Thus, the energy criterion f_E is defined as the average number of emissions and reception operations performed by all nodes (sources and relays). This value is normalized by the number of frames sent by the sources. The complete definition is given in [9].

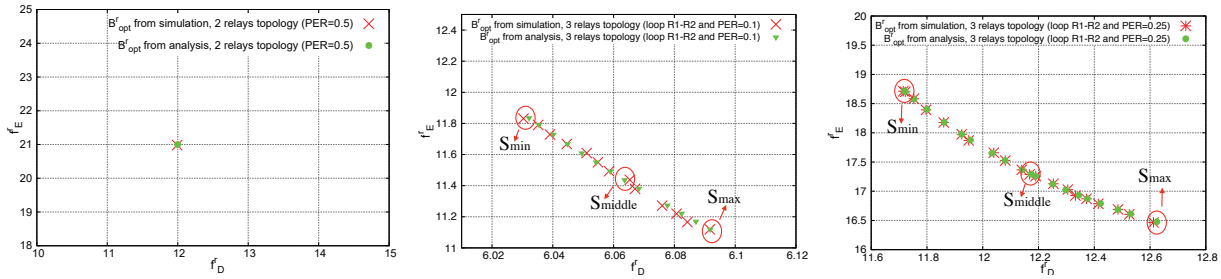

(a) Pareto optimal bound for 2-flow 2-relay wireless networks (b) Pareto optimal bound for 1-flow 3-relay wireless networks (c) Pareto optimal bound for 1-flow 3-relay wireless networks

Fig. 3. Reliability-achieving Pareto optimal bounds. x-axis (resp. y-axis) represents the average duration in milliseconds (resp. in Joules) for one frame received at the destination, where forwarding probability value chosen in set [0,1].

IV. MO OPTIMIZATION PROBLEM

The resource allocation we propose in this paper is obtained by selecting the forwarding probabilities of all relays by solving the MO optimization problem introduced hereafter. This problem concurrently minimizes the Reliability-achieving end-to-end delay and Reliability-achieving energy metrics. Both metrics are introduced first.

A. Reliability-achieving criteria

Previously defined end-to-end delay and energy metrics are normalized by the reliability criterion f_R. As such, we derive metrics that measure the end-to-end delay and energy it would cost to achieve a perfectly reliable communication. Formally, they are defined for one flow arriving at destination D_j by:

Reliability achieving delay f_D^r:

$$f_D^r(D_j) = f_D(D_j)/f_R(D_j) \tag{12}$$

Reliability achieving energy f_E^r:

$$f_E^r(D_j) = f_E(D_j)/f_R(D_j) \tag{13}$$

A global metric is proposed that combines the performance of all flows:

$$f_D^r = \max_{j\in|\mathcal{D}|} f_D^r(D_j) \quad \text{and} \quad f_E^r = \frac{1}{|\mathcal{D}|}\sum_{j=1}^{|\mathcal{D}|} f_E^r(D_j) \tag{14}$$

The maximum end-to-end delay over all flows is minimized in f_D^r and the average energy consumption is minimized in f_E^r.

B. MO Optimization problem

In our MO problem, we optimize the forwarding probabilities represented by $X \in \mathcal{X}^\tau$. Each solution $X \in \mathcal{X}^\tau$ can be evaluated according to f_R, f_D or f_E. In this paper, the following multi-objective optimization problem is solved:

$$\begin{aligned} & [\min f_D^r(x), \min f_E^r(x)]^T \\ s.t. \quad & x = (\tau, X) \in \Gamma \times \mathcal{X}^\tau \end{aligned} \tag{15}$$

In this work, we define a Pareto-optimal reliability-achieving bound $\mathcal{B}_{opt}^r$ by the set of points given by

$$\mathcal{B}_{opt}^r = \{(f_D^r(x), f_E^r(x)) \ \forall x \in \mathcal{S}_{opt}\}$$

This bound and $\mathcal{S}_{opt}$ are obtained by solving (15), with $\mathcal{S}_{opt}$ the set of Pareto-optimal solutions. Each solution is defined by the values of the forwarding probabilities of the relay nodes. Two different implementations are studied in this work. The first one looks for binary values. In this case, the schedules obtained after MO optimization are deterministic. The second implementation looks for real-valued probabilities that belong to the [0,1] continuous set. Schedules are as such stochastic and each relay runs Algorithm 1 using a set of Pareto-optimal forwarding probabilities.

V. RESULTS

Deterministic and stochastic schedules are computed for the topologies of Fig. 1. For the deterministic schedule derivation, no cycles are allowed (reverse path forwarding probabilities are set to 0). For the stochastic schedule derivation, one loop may be exploited by our framework. For both approaches, stochastic worst-case delay bounds are presented to exhibit how our framework can be leveraged for certification purposes. Imperfect channel conditions are mostly considered to highlight the impact of cyclic paths on the overall performance.

A. Simulation settings

1) Network settings: Results are given assuming an Additive White Gaussian Noise (AWGN) channel and a Binary Phase Shift Keying (BPSK) modulation without coding providing a bit error rate of $BER(\gamma) = Q(\sqrt{2\gamma}) = 0.5 * \text{erfc}(\sqrt{\gamma})$, with γ the per bit signal to noise and interference ratio experienced on the link and $erfc$ the complementary error function. For a specific value of SINR γ, the packet error rate PER is computed with $PER(\gamma) = 1 - [1 - BER(\gamma)]^{N_b}$ where N_b is the number of bits of a data frame. Any channel model can be exploited in our framework.

Interference is accounted for in our channel model if two relays or more are chosen to forward frames in the same cell by our optimization search. For instance, for the 1-flow 3-relay topology, we have $|\mathcal{T}| = 4$ time-frequency blocks to allocate. In our search, source S can only transmit in cell 1, R_1 may transmit in cell 2 or 3; relay R_2 in cell 3 or 4; and relay R_3 in cell 3 or 1. For the 2-flow topologies, $|\mathcal{T}| = 4$ time-frequency block have to be allocated as well. The sources S_1 and S_2 only emit in cell 1 and 2, respectively. The relay R_1 may transmit in block 3 or 4; and relay R_2 in block 4 or 1.

For all topologies, the results are given for a slotframe duration of 3 slots. With 2 channels, there are hence 6 cells in

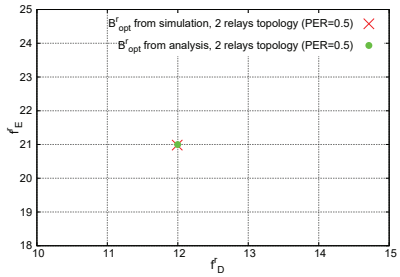

(a) Pareto optimal bound for 2-flow 2-relay

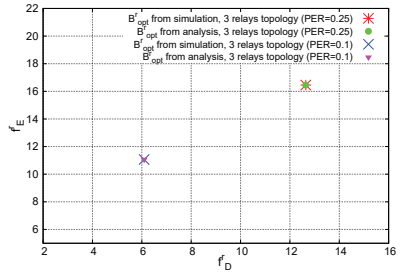

(b) Pareto optimal bound for 1-flow 3-relay

Fig. 4. Pareto optimal bound for all topologies for different d_{onehop}, where forwarding probability chosen integer 0 or 1.

the schedule. Moreover, all nodes are perfectly synchronized. The time-frequency block is of $\varsigma_{slot} = 10$ms, the regular slot duration of IEEE802.15.4e. Note that this duration is long enough to carry a frame with payload of 127 bytes using IEEE802.15.4e at 250kbps.

2) MO optimization: $\mathcal{S}_{opt}$ and $\mathcal{B}^r_{opt}$ are derived using NSGA-2 for a population size of 300 solutions, 1000 generations and a crossover probability of 0.9. A transmission power $P_T = 0.15$mW and a pathloss exponent of 3 is considered. For any time-frequency block $u \in \mathcal{T}$, there is an interference-limited channel between any two nodes i and j of the network.

For all considered topologies, relay locations are defined. An imperfect channel is considered by setting the 1-hop distance d_{onehop} to 340.75m, 324.58m or 357.8m to create a 1-hop transmission with a Packet Error Rate of $PER = 0.25$, $PER = 0.1$ and $PER = 0.5$, respectively. Nodes located at a two-hop distance are out of reach.

Wireless topologies and protocols are simulated using the realistic discrete event-driven network simulator WSNet[1]. In all topologies, sources only generate frames and destinations only receive them. The sources emit a periodic flow of frames whose period is set differently according to the protocol in use. The end-to-end delay is the duration between the arrival of the frame in the source buffer and the arrival of the frame in its destination buffer. Frames have a size of 127 bytes of payload (i.e. the standard maximum IEEE802.15.4 frame size). Simulations are performed for the duration necessary to complete the transmission of 100 000 frames.

3) Results assessment: To measure the closeness of Pareto sets computed analytically and by simulations, two metrics are calculated : the root mean squared error (RMSE) and the Generational Distance (GD). $RMSE = \frac{1}{n}\sqrt{\sum_{i=1}^{n} \frac{(d(i)-\tilde{d}(i))^2}{f(i)^2}}$, with n the total number of points in the set, $d(i)$ and $\tilde{d}(i)$ the analytical and simulated reliability-achieving end-to-end delay and energy values. The generational distance is defined by $GD = \frac{1}{N_{opt}}\left(\sum_{i=1}^{N_{opt}}(d_i^p)\right)^{1/p}$ with d_i the Euclidian distance between analytical and simulated bounds. We use $p = 2$.

[1] http://wsnet.gforge.inria.fr/

TABLE I. RMSE AND GD FOR PARETO OPTIMAL BOUNDS

	f^r_D	f^r_E	GD
1-flow 3-relay	$9.76 * 10^{-5}$	$7.30 * 10^{-5}$	$1.74 * 10^{-3}$
2-flow 2-relay	$3.47 * 10^{-5}$	$7.07 * 10^{-5}$	$8.50 * 10^{-5}$

B. Pareto bounds

Table I lists RMSE and GD values for the two considered topologies. Values are really small, showing a quasi-perfect match between the model and simulations. Bounds are presented in the following for both deterministic and stochastic schedule derivations.

C. Deterministic schedule

For all investigated topologies, the optimal binary forwarding probabilities and evaluation criteria are given in Table II. The binary values have been derived by solving the multi-objective optimization problem of Eq. (15). For this scenario, the bound resumes to a single trade-off value.

1) 2-flow / 2-relay topology: For the 2-flow / 2-relay scenario, optimal forwarding probabilities and criteria are shown in Table II. The Pareto set is represented in Fig. 4(a) for $d_{\text{onehop}} = 357.8m$ ($PER = 0.5$). For this simple scenario, the whole search has resumed to a single Pareto-optimal point. Since it is a symmetric topology, the criteria for the flow ending at D_1 is the same as for the one ending at D_2. Since there is only one path from S_1 to D_1, the number of hops travelled by frames to reach their destination is always equal to 3.

2) 1-flow 3-relay: For the 3-relay scenario, two different channels are investigated for $PER = 0.25$ et $PER = 0.1$. As shown in Fig. 4(b), not surprisingly, the Pareto bound $PER = 0.1$ dominates the solution with the higher PER ($PER = 0.25$). Optimal forwarding probabilities and criteria as shown in Table II.

D. Stochastic schedule

The Pareto-optimal forwarding probabilities for the stochastic study are given in Table II for both topologies. For the 1-flow / 3-relay topology, only one loop is allowed in the search between R_1 and R_2. Forwarding probabilities are searched in a discrete set $[0, 0.01, \ldots, 1-\Delta]$ of step 0.01.

1) 2-flow / 2-relay topology: As seen in Table II, Pareto-optimal solutions have a non-zero forwarding probability When $d_{\text{onehop}} = 357.8m$ ($PER = 0.5$), the whole search has resumed to a single Pareto-optimal point as represented in Fig. 3(a). The optimal forwarding probabilities and criteria are shown in Table II. We can see that the Pareto bounds and forwarding probability values are the same as the ones obtained for a deterministic schedule.

TABLE II. DETERMINISTIC SCHEDULE (BINARY FORWARDING PROBABILITIES) AND CRITERIA FOR ALL CONSIDERED TOPOLOGIES.

2-flow / 2-relay scenario ($d_{\text{onehop}} = 357.8$ (1-PER = 0.5))									
$x^{13}_{S_1R_1}$	$x^{14}_{S_1R_2}$	$x^{23}_{S_2R_1}$	$x^{24}_{S_2R_2}$	$x^{34}_{R_1R_2}$	$f_R(D_{1\|2})$	$f_D(D_{1\|2})$	$f_E(D_{1\|2})$	f^r_D	f^r_E
1	0	1	0	1	0.25	3	5.25	12	21

1-flow / 3-relay scenario ($d_{\text{onehop}} = 340.75$ (1-PER = 0.75))										
$x^{12}_{SR_1}$	$x^{13}_{SR_2}$	$x^{14}_{SR_3}$	$x^{23}_{R_1R_2}$	$x^{24}_{R_1R_3}$	$x^{34}_{R_2R_3}$	$f_R(D)$	$f_D(D)$	$f_E(D)$	f^r_D	f^r_E
1	0	0	1	0	1	0.3165	4	5.2074	12.6398	16.4551

1-flow / 3-relay scenario ($d_{\text{onehop}} = 324.58$ (1-PER = 0.9))										
$x^{12}_{SR_1}$	$x^{13}_{SR_2}$	$x^{14}_{SR_3}$	$x^{23}_{R_1R_2}$	$x^{24}_{R_1R_3}$	$x^{34}_{R_2R_3}$	$f_R(D)$	$f_D(D)$	$f_E(D)$	f^r_D	f^r_E
1	0	0	1	0	1	0.6561	4	7.2632	6.0965	11.0700

TABLE III. STOCHASTIC SCHEDULE AND CRITERIA FOR ALL CONSIDERED TOPOLOGIES.

2-flow / 2-relay scenario ($d_{\text{onehop}} = 357.8$ (1-PER = 0.5))										
	$x^{13}_{S_1R_1}$	$x^{14}_{S_1R_2}$	$x^{23}_{S_2R_1}$	$x^{24}_{S_2R_2}$	$x^{34}_{R_1R_2}$	$f_R(D_{1\|2})$	$f_D(D_{1\|2})$	$f_E(D_{1\|2})$	f^r_D	f^r_E
Unique Solution	1	0	1	0	1	0.25	3	5.25	12	21

1-flow / 3-relay scenario ($d_{\text{onehop}} = 340.75$ (1-PER = 0.75) and loop between R_1 and R_2)												
	$x^{11}_{SR_1}$	$x^{23}_{R_1R_2}$	$x^{24}_{R_1R_3}$	$x^{32}_{R_2R_1}$ (loop)	$x^{34}_{R_2R_3}$	$x^{42}_{R_3R_1}$	$x^{43}_{R_3R_2}$	f_R	f_D	f_E	f^r_D	f^r_E
S_{min}	1	1	0	0.59	1	0	0	0.3704	4.3411	6.9338	11.7191	18.7183
S_{middle}	1	1	0	0.3	1	0	0	0.3417	4.1594	5.9094	12.1732	17.2947
S_{max}	1	1	0	0.01	1	0	0	0.3183	4.0049	5.227	12.6242	16.4763

1-flow / 3-relay scenario ($d_{\text{onehop}} = 324.58$ (1-PER = 0.9) and loop between R_1 and R_2)												
	$x^{12}_{SR_1}$	$x^{23}_{R_1R_2}$	$x^{24}_{R_1R_3}$	$x^{32}_{R_2R_1}$ (loop)	$x^{34}_{R_2R_3}$	$x^{42}_{R_3R_1}$	$x^{43}_{R_3R_2}$	f_R	f_D	f_E	f^r_D	f^r_E
S_{min}	1	1	0	0.137	1	0	0	0.6702	4.0431	7.9327	6.0322	11.8354
S_{middle}	1	1	0	0.08	1	0	0	0.6643	4.0249	7.6348	6.0589	11.4931
S_{max}	1	1	0	0.01	1	0	0	0.6571	4.0031	7.3070	6.0917	11.1195

2) 1-flow / 3-relay topology: In this scenario, only one cyclic path is allowed in the search between R_1 and R_2. More specifically, the forwarding probabilities $x^{uv}_{21}, \forall u, v$ are part of the optimization variables. Two different channel conditions are tested as well, naming $PER = 0.25$ et $PER = 0.1$. Three forwarding solutions S_{min}, S_{middle} and S_{max} are investigated for each case as shown in Table II, all extracted from the Pareto-optimal set of Fig. 3(b) and Fig. 3(c). The first one, S_{min}, exhibits the smallest average end-to-end delay (but the highest average energy), the second one, S_{max}, exhibits the largest average end-to-end delay (but the smallest average energy) and the last one, S_{middle} an average delay in between smallest and largest. As seen in Table II, optimal Pareto solutions have a non-zero loop forwarding probability ($x^{32}_{R_2R_1}$). This clearly shows that best solutions benefit from this additional redundancy, when both delay and energy are optimized concurrently. For $PER = 0.25$, the forwarding probability is of $x^{32}_{R_2R_1} = 0.59$ in S_{min}, while for $PER = 0.1$, the forwarding probability is of $x^{32}_{R_2R_1} = 0.137$ in S_{min}. For the better link quality, the forwarding probability is smaller than for the worst link quality. This loop clearly compensates for channel frame losses. Compared to binary schedules, stochastic schedules create a Pareto bound that dominates the binary Pareto sets. In other words, stochastic schedules are performing better than binary ones. This is an important feature where we highlight that cyclic paths are beneficial in this context.

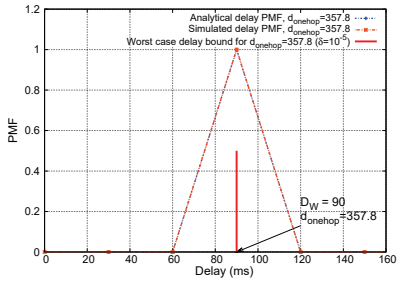

(a) 2-flow / 2-relay

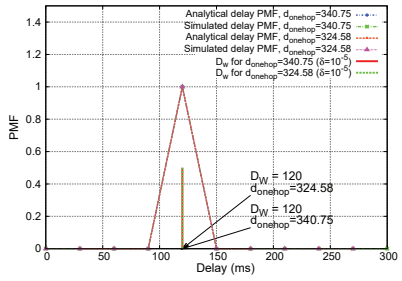

(b) 1-flow / 3-relay

Fig. 5. PMF of delay for different PER - slot duration of 10ms and binary Pareto-optimal schedule.

E. Delay distribution and Worst-case delay bound

Delay distribution and worst case delay bounds for binary and stochastic forwarding probabilities are given next.

a) Deterministic schedule: For the 1-flow / 3-relay and 2-flow / 2-relay networks, since there is only one path from source to destination, the end-to-end delay and the worst case delay are equal to a fixed value as shown in Fig. 5(a) and Fig. 5(b). The analytical delay distribution for one source-destination pair matches well with the simulation results. As shown in Table IV, that shows the impact of the number of relays N on the linear topology, the worst case delay bound grows with N.

b) Stochastic schedule: As seen in Fig. 6, the analytical delay distribution for one source-destination pair compared

TABLE IV. D_W FOR ALL TOPOLOGIES, WHERE FORWARDING PROBABILITY INTEGER 0 OR 1.

	δ	D_W ($\varsigma_{slot} = 10$ms)
2-flow 2-relay	10^{-5}	90 (3 hops)
1-flow 3-relay	10^{-5}	120 (4 hops)

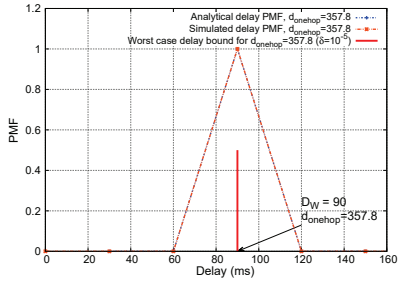

(a) 2-flow / 2-relay with the unique Pareto-optimal solution

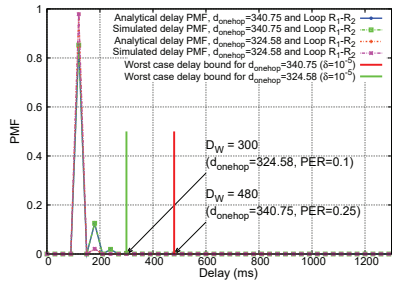

(b) 1-flow / 3-relay with Pareto-optimal solution S_{min}

Fig. 6. PMF of delay for different PER and slot duration of 10ms using stochastic schedules

with the simulation results for all considered networks match well. For the 1-flow / 3-relay TDMA networks, there are several Pareto solutions. We recall that we have picked three Pareto optimal solutions to show their delay distribution: S_{min}, S_{middle} and S_{max}. Their respective distributions are plotted in Fig. 6(b) for 1-flow 3-relay network. The tail of the distribution is very difficult to validate with simulations since such delays are very rare events, with very small probabilities. However, the overall fit is really close and the RMSE between analytical and simulated delay PMF for the 3-relay TDMA network confirms this statement: the RMSE is of $4.83 * 10^{-3}$ for S_{min}, $1.06 * 10^{-4}$ for S_{middle} and of $9.81 * 10^{-4}$ for S_{max}. Again, these values are really small which confirms the validity of our model.

Looking at worst case delays for 1-flow 3-relay in Table V, the value of D_w clearly increases with the PER. It higher accuracies are required, the larger the D_w values get.

VI. Conclusions

In this paper, we propose a certifiable resource allocation for real-time multi-hop 6TiSCH wireless network. This framework calculates offline a schedule that can be deterministic (binary forwarding probabilities) or stochastic (real-valued forwarding probabilities). We further certify the applicability of our algorithm to real-time communications by calculating stochastic worst-case delay bounds for considered topologies and flow patterns. The results shows that stochastic forwarding probability improves overall performance compared to the deterministic scheduling with binary values. It is interesting and important because a node doesn't always use the same channel and slot (superframe changes over time) - messages don't always take same path. Introducing the loop probability can even further help by adding path diversity and thus offer higher robustness. Our offline resource allocation calculation is not flow-dependent: there is no variable per flow, we work on an aggregated view of all flows in the network (not a too fine grained calculation of emission decisions), which is better when we want to model a flow envelope and not the exact detail of how it is created.

TABLE V. D_W FOR FORWARDING PROBABILITY CHOSEN IN SET [0,1], GIVEN FOR S_{min} SOLUTION (UNIT: MS).

	δ	D_W (ς_{slot} = 10ms)
2-flow 2-relay	10^{-5}	90 (3 hops)
1-flow 3-relay (PER=0.25 Loop R_1-R_2)	10^{-5}	480 (16 hops)
	10^{-7}	660 (22 hops)
	10^{-9}	780 (26 hops)
1-flow 3-relay (PER=0.1 Loop R_1-R_2)	10^{-5}	300 (10 hops)
	10^{-7}	420 (14 hops)
	10^{-9}	480 (16 hops)

VII. Acknowledgments

This work was supported in part by the National Natural Science Foundation of China (NSFC) under Grant No. 61602447.

References

[1] "WirelessHART Specification 75, TDMA Data-Link Layer, HART Communication Foundation Standard hCF SPEC-75," 2008.1.1.

[2] S. Petersen and S. Carlsen, "WirelessHART Versus ISA100.11a: The Format War Hits the Factory Floor," *Industrial Electronics Magazine, IEEE*, vol. 5, no. 4, pp. 23–34, Dec 2011.

[3] "IEEE Standard for Local and Metropolitan Area Networks—Part 15.4 Low-Rate Wireless Personal Area Networks (LR-WPANs) Amendment 1: MAC Sublayer," *IEEE Standard 802.15.4e-2012*, Apr. 2012.

[4] Q. Wang, X. Vilajosana, and T. Watteyne, "6tisch operation sublayer (6top)," *IETF Standard draft-wang-6tisch-6top-sublayer-01*, Jul. 2014.

[5] M. Domingo-Prieto, T. Chang, X. Vilajosana, and ThomasWatteyne, "Distributed pid-based scheduling for 6tisch networks," *IEEE COMMUNICATIONS LETTERS*, vol. 20, no. 5, pp. 1006–1009, May 2016.

[6] S. Duquennoy, B. A. Nahas, O. Landsiedel, and T.Watteyne, "Orchestra: Robust mesh networks through autonomously scheduled tsch," in *in Proc. Embedded Netw. Sensor Syst. (SenSys)*, Nov. 2015, pp. 337–350.

[7] I. Hosni, F. Theoleyre, and N. Hamdi, "Localized scheduling for end-to-end delay constrained low power lossy networks with 6tisch," in *IEEE ISCC*, 2016.

[8] Q. Wang, K. Jaffrès-Runser, C. Goursaud, J. Li, Y. Sun, and J.-M. Gorce, "Deriving pareto-optimal performance bounds for 1 and 2-relay wireless networks," in *IEEE IC3N*, Nassau, Bahamas, August 2013.

[9] Q. Wang, K. Jaffres-Runser, Y.-J. Xu, J.-L. Scharbarg, Z.-L. An, and C. Fraboul, "TDMA versus CSMA/CA for wireless multi-hop communications: a stochastic worst-case delay analysis," *IEEE Transactions on Industrial Informatics*, vol. PP, no. 99, 2016.

[10] Q. Wang, K. Jaffrès-Runser, Y.-J. Xu, J.-L. Scharbarg, Z.-L. An, and C. Fraboul, "TDMA versus CSMA/CA for wireless multi-hop communications: A comparison for soft real-time networking," in *IEEE WFCS*, 2016.

[11] "Part 15.4: Wireless Medium Access Control (MAC) and Physical Layer (PHY) Specifications for Low-Rate Wireless Personal Area Networks (LR-WPANs)," *IEEE Standard 802.15.4*, 2011.